Aerosol Science and Technology 36: 642–651 (2002)

Published by Taylor and Francis
0278-6826/02/$12.00 + .00

The Use of STIM and PESA to Measure Profiles of Aerosol Mass and Hydrogen Content, Respectively, across Mylar Rotating Drums Impactor Samples

Graham Bench,[1] Patrick G. Grant,[1] Dawn Ueda,[1] Steve S. Cliff,[2] Kevin D. Perry,[3] and Thomas A. Cahill[2]

[1] *Center for Accelerator Mass Spectrometry, Lawrence Livermore National Laboratory, Livermore, California*
[2] *Department of Land, Air and Water Resources (LAWR), University of California, Davis, California*
[3] *Department of Meteorology, San Jose State University, San Jose, California*

A method has been developed for measuring profiles of aerosol mass on thin (480 μg/cm^2) Apiezon-L coated Mylar films employed in rotating drum aerosol impactor samplers using the ion beam analysis technique scanning transmission ion microscopy (STIM). The greased Mylar films are excellent impaction substrates and possess excellent uniformity in projected density, making them an ideal substrate for STIM analysis. The uniformity in projected density of a film enables STIM with a 3 MeV proton beam to produce profiles of aerosol mass with an accuracy of better than 90% and a mass sensitivity approaching 10 μg/cm^2. Further, we have extended proton elastic scattering analysis (PESA) to the same films, achieving measurement of an organic surrogate. Although the films contain ~ 20 μg/cm^2 hydrogen, the spatial uniformity in film hydrogen content enables PESA with a 3 MeV proton beam to produce profiles of hydrogen arising solely from the aerosols with an accuracy to within ± 1 μg/cm^2 and a mass sensitivity of ~ 1 μg/cm^2. These measurements when combined with synchrotron-x-ray fluorescence (S-XRF) measurements on the same film allow mass closure, sum of species versus measured mass, a key quality assurance protocol, to be approached. All 3 techniques were applied to very fine and ultra-fine particles collected in Fresno, CA, November, 2000 by slotted DRUM samplers. Temporal resolution in the resulting profiles was ≤ 6 h. The dramatic changes in composition versus size and time, and new types of elemental correlations unseen in PM$_{2.5}$ filters, will be major assets in correlating aerosols and health impacts, visibility degradation, and the effects of aerosols on climate.

Received 27 June 2001; accepted 13 August 2001.

This work was partially supported by a NSF grant ATM-0080225 and was partially performed under the auspices of the U.S. Department of Energy by Lawrence Livermore National Laboratory under contract W-7405-ENG-48.

We would like to acknowledge Dr. Nehzat Motellabi and the California Air Resources Board for their invaluable assistance and support in the FACES study and our efforts to advance size and time resolved sampling for health studies.

Address correspondence to Graham Bench, Center for Accelerator Mass Spectrometry, L-397, Lawrence Livermore National Laboratory, Livermore, CA 94550. E-mail: bench1@llnl.gov

INTRODUCTION

Compositional analysis of aerosols is greatly aided by removing the particles from the overwhelming volume of carrier gases. Separation of aerosols from the ambient atmosphere by impaction offers many advantages over standard filtration techniques. Some of the most important advantages are the ability of impactors to segregate by particle size, to better preserve chemical integrity since the air stream does not pass through the deposit, to collect samples as a function of time, and to have a wide variety of impaction surfaces available to match analytical needs. Disadvantages include the increased analytical costs associated with size-segregated samples, the very small amount of mass available for compositional analysis, and the difficulty in measuring the mass of the deposit (Cahill and Wakabayashi (1993) and references therein). For impactor strips that have sampled aerosols as a function of time, spatially small areas (as small as 0.2 × 0.2 mm) have to be studied on the strip that has typical dimensions of ~1 × 15 cm. The collected aerosol mass in a given area is sufficiently small (on the order of 100 μg/cm^2) and covers a sufficiently small area that measurement of total mass in such an area has rarely been achieved (Malm et al. 1994). While impaction has been used since the 1970s, the lack of mass has become a major handicap for integration of impaction-based studies into standard EPA filter based mass standards. As an example, data from 14,400 days of 3 size cut impaction based air monitoring in California, 1973–1977 (Flocchini et al. 1976), was useful for many purposes (Barone et al. 1978), but was not able to account for more than about 20% of the aerosol mass seen on side by side samples. It was also not possible to measure total

mass directly from the impaction strips. Furthermore, this study had no capability for organic and nitrate mass determination. This was primarily due to the inability of x-ray based methods to measure organic matter and nitrates (Cahill et al. 1989).

In this paper, we report on developing and/or extending methods that measure both total mass and organic matter mass surrogates thus allowing us to approach mass closure, which is so important to quality assurance protocols in speciated aerosols. Measurement of total mass involves the use of the well-established method of scanning transmission ion microscopy (STIM) (Lefevre et al. 1987; Bench et al. 1993) on aerosol strip samples from impactors. The strip sample substrate used was Apiezon-L coated Mylar. This substrate has excellent particle collection and antibounce capabilities and we show that it has excellent uniformity in projected density, making it a suitable substrate for STIM analysis. Further, the well-established proton elastic scattering analysis (PESA) method (Cahill et al. 1987; Malm et al. 1994; Cohen et al. 1996) has been extended to the same substrates. PESA has routinely been used to measure aerosol hydrogen content on Teflon substrates (which are hydrogen free) to deliver a surrogate organic composition. Here we show that although the Mylar substrate has a large hydrogen blank value, the hydrogen content of this substrate is relatively uniform. This uniformity allows reliable subtraction of the substrate hydrogen yield from the sample hydrogen yield to give aerosol hydrogen content for determination of an organic surrogate. Finally we show how STIM and PESA measurements when combined with synchrotron-x-ray fluorescence (S-XRF) measurements on the same foil allow us to employ the concept of integral redundancy to approach mass closure, sum of species versus measured mass. All 3 techniques were applied to very fine and ultra-fine particles collected in Fresno, CA, November, 2000 with slotted DRUM samplers (Raabe et al. 1988). It is not the purpose of this paper to present a detailed analysis of ambient aerosols of Fresno. However, the STIM, PESA, and S-XRF analyses of the impaction strips revealed dramatic changes in composition versus size and time and new types of elemental correlations unseen in $PM_{2.5}$ filters. The wealth of information obtained suggests that data acquired from the STIM, PESA, and S-XRF analyses of impaction strips could be a major asset in correlating aerosols and health impacts, visibility degradation, and the effects of aerosols on climate.

METHODS

Samples

The rotating drum impactor substrates were $\sim 1 \times 17$ cm^2 strips of Apiezon-L (M & I Materials Limited, Manchester, U.K.) coated Mylar ($C_{10}H_8O_4$) with an areal density of $\sim 480 \pm 10$ μg/cm^2. The 480 μg/cm^2 Mylar strips were coated with ~ 5 μg/cm^2 Apiezon-L in the laboratory after purchase by uniformly exposing the Mylar strips to a 2% by weight solution of Apiezon-L in toluene. Coating thickness was determined by weighing the strip before and after coating. Apiezon-L grease is a clean, high poise vacuum grease shown to have excellent antiparticle bounce capabilities (Wesolowski et al. 1978; Cahill 1979). For the work reported here, aerosol samples were collected at the Fresno, CA, EPA Superfund site from November 8 through 29, 2000 for the California Air Resources Board as part of the preliminary quality assurance tests for the Fresno Asthmatic Children Environment Study (FACES). This paper reports on STIM, PESA, and S-XRF analysis of 6 sub $PM_{2.5}$ (particles with aerodynamic diameter ≤ 2.5 μm) mode stages from the rotating drum aerosol impactor studies in Fresno—stages 3–8. These 6 stages represent particulate aerodynamic diameters (D_p) in the following size ranges: 2.5 μm $> D_p \geq 1.15$ μm (stage 3), 1.15 μm $> D_p \geq 0.75$ μm (stage 4), 0.75 μm $> D_p \geq 0.56$ μm (stage 5), 0.56 μm $> D_p \geq 0.34$ μm (stage 6), 0.34 μm $> D_p \geq$ 0.24 μm (stage 7), and 0.24 μm $> D_p \geq 0.07$ μm (stage 8). These cut points differ from the original cut points of the jetted DRUM sampler (Raabe et al. 1988) since they were modified when the unit was changed from single jets to 6 mm long slots (Raabe 1997). The rotating DRUM impactor strips had a rotation rate of 4 mm/day sampling a flow of 10 L/min through a 6 mm length slot. Four blank Apiezon-L coated Mylar strips were also examined via STIM and PESA to determine the contribution of the film to the energy lost by the proton beam and the hydrogen yield.

Nuclear Microprobe Sample Orientation and Scanning

Samples were analyzed at the nuclear microprobe facility at the Lawrence Livermore National Laboratory (Roberts et al. 1999) using PESA and STIM to determine the profiles of aerosol hydrogen content and projected density, respectively, along each sample. Because STIM utilizes a millionfold lower beam currents than PESA, all samples were initially analyzed by STIM. For all analyses an incident 3 MeV proton beam was focused onto the specimen in a square spot of size 125×125 μm^2. Samples were mounted within the microprobe target chamber with the largest dimension in the vertical direction. The sample surface was normal to the incident beam direction and oriented so that any deposited aerosol was facing downstream from the incident beam. With this orientation the beam passes through the substrate before the aerosol and always loses the same amount of energy in passing through a uniform substrate, independent of variations in the amount of aerosol on the substrate.

To obtain spatial information, the beam was scanned over the sample and data recorded as a function of beam position. Owing to the spatial extent of the samples, sample scanning was achieved by a combination of electrostatic and mechanical scanning. Electrostatic scanning of the incident beam was utilized to scan areas of 1×1 mm^2 using a point by point raster mode with a pixel (or step) size of 125 μm. The beam dwelt at a particular sample location until a preset amount of integrated charge was recorded before stepping onto the next beam location. Following completion of an electrostatic scan the

sample was mechanically translated vertically 1 mm and another electrostatic scan started. This process was repeated until the desired length of the sample to be analyzed had been achieved. The whole process is automated and with this approach samples as long as 20 cm can be analyzed. However, the 6 FACES sub $PM_{2.5}$ mode drum impactor samples had only been exposed to aerosol material along ~9 cm of the sample length (corresponding to the time period of November 8 to 29, 2000). Consequently, scan sizes of 1 × 90 mm were utilized to scan all samples. These scans consisted of 8 × 720 pixels with a pixel size of 125 × 125 μm^2. The vertical step size of 125 μm in the STIM and PESA profiles corresponds to an impactor drum collection time period of 0.75 h for the FACES samples. In addition, to determine the reproducibility of the STIM and PESA data collection and analysis protocols the FACES stage 8 sample was analyzed in 2 separate 1 mm × 90 mm areas laterally separated by 2 mm. As the length of the impactor slot was ~6 mm, ~16% of the aerosols collected on a strip were measured in an individual profile.

STIM Data Collection and Reduction

To determine profiles of aerosol mass or areal density on a sample, a method that can resolve <50 $\mu g/cm^2$ aerosol areal density differences within localized areas on a sample is required. STIM can supply such data by measuring the energy lost by the incident beam as it traverses the sample (Lefevre et al. 1987). Protons with energies above 1 MeV primarily lose energy in passing through a specimen by interactions with specimen atom electrons. Because of the simple physics involved in this ion energy loss mechanism and the accurate data bases available, ion energy losses can be readily converted into specimen projected densities which in turn can be used to determine specimen mass (Lefevre et al. 1987, 1991; Bench et al. 1993). STIM has previously been used to determine the areal densities of thin material films of known areal density and composition (Bench 1991). Conversion of energy losses to areal densities using the known material composition revealed the technique to have a quantitative accuracy of better than 95% in determining sample areal densities (Bench 1991).

Residual proton energies after traversing the sample were measured with a 300 mm^2 retractable charged particle silicon surface barrier detector located ~5 cm directly behind the sample. To avoid catastrophic damage to the detector with the nanoampere beam currents used with most other microprobe analysis techniques, beam currents of 2,000 protons per second (~3×10^{-16} A) were used for STIM analysis by reducing the size of an aperture just after the ion source. Restricting this aperture affords fine control of the amount of beam current incident on target over a range of nanoamperes down to a few ions per second and has no noticeable effect on the final beam spot size. With STIM, as virtually every incident ion produces useful information in traversing the sample, the technique is nearly 100% efficient (Lefevre et al. 1991), consequently, even with low beam currents data acquisition is rapid. The STIM data sets reported here took ~20 min to acquire.

Residual ion energies were recorded in list mode along with coincident beam spatial coordinates arising from scanning the beam over the sample. The residual energy of 199 ions was measured at each beam location. The median value of these 199 ion energies was selected to represent the average residual energy of the ion beam at each beam location (Lefevre et al. 1987). The product of STIM data collection was a two-dimensional data set (8 × 720 pixels) of the median residual ion energy at each beam location on the sample. Inspection of each data set showed that for a given vertical position the resulting median residual ion energies for each horizontal position were similar. Consequently, before further analysis the median STIM data values in a data set were averaged over the horizontal direction and the resulting energies converted to energy losses. This process resulted in a linescan of ion energy loss versus position across the sample consisting of 720 data points with a spacing of 125 μm between sequential points. Each data point represented an interrogated area of 125 μm by 1 mm.

STIM energy loss data from the 6 FACES sub $PM_{2.5}$ mode samples were corrected for the Mylar film contribution to the energy loss by subtracting the measured energy thickness of the blank films to produce profiles of energy loss arising solely from the aerosols. Aerosol energy losses were converted to areal densities using the annual average <2.5 μm diameter aerosol composition for Sequoia National Park, CA (Malm et al. 1994), shown in Table 1 and a beam energy that had been corrected for

Table 1
Fractional weights for the 18 most common elements found in the <2.5 micron diameter annual average aerosol composition at Sequoia National Park

Element	Fractional weight (g/g)
H	0.0340
C	0.2131
N	0.0822
O	0.4737
Na	0.0180
Si	0.0881
S	0.0337
Cl	0.0013
K	0.0133
Ca	0.0113
Ti	0.0027
V	0.0002
Mn	0.0005
Fe	0.0270
Cu	0.0001
Zn	0.0003
Br	0.0002
Pb	0.0001

energy loss after passing through the Mylar film. The aerosol composition from Sequoia National Park strongly reflects the San Joaquin Valley within which Fresno is located.

PESA Data Collection and Reduction

With PESA, protons with energies above 1 MeV that elastically scatter from target atoms into forward angles can be detected by a particle detector (Cahill et al. 1987). The energy of the scattered projectiles depends on the atomic number of target atoms. By measuring the energy of the scattered ions it is possible to discriminate ions scattered from hydrogen from ions scattered by other elements. Integrating the number of ions scattered from hydrogen gives a quantitative measure of the sample hydrogen content. Forward scattered protons were detected with a silicon surface barrier charged particle detector that subtended a solid angle of $\sim 75 \times 10^{-3}$ steradian to the specimen. The detector was located at an angle of 45° with respect to the incident beam. Total incident beam charge was collected in a Faraday cup located 15 cm behind the sample.

As the beam was scanned across the sample, PESA data were recorded in list mode along with coincident beam spatial coordinates arising from scanning the beam over the sample. Beam currents were in the range of 1.5 to 2.5 nA and 1 nC was deposited to each beam location. PESA data sets typically took ~55 min to acquire. The data were then sorted off-line into a data cube with axes energy, horizontal position, and vertical position. Inspection of each cube showed that for a given vertical position the resulting PESA spectra for each horizontal position were virtually identical. Consequently, before further analysis PESA spectra were summed across the horizontal direction to improve counting statistics. The result of this compression produced a two-dimensional data set with axes of energy and position, a step size of 125 μm, and an interrogated area in each step of 125 μm by 1 mm. The number of ions scattered from hydrogen at each position ordinate in this data set was computationally calculated by setting a window around the hydrogen peak, integrating the number of counts within this window, and subtracting any contribution from the background continuum. Because backgrounds underneath the hydrogen peak were low and displayed a roughly linear increase with increasing ion energy, a linear fit to the background on either side of the hydrogen peak was used to determine the background contribution. Thin plastic films with known hydrogen contents of 10, 50, and 100 μg/cm^2 were analyzed via PESA to generate a linear calibration curve of hydrogen yield versus hydrogen areal density. This calibration curve was used to convert strip sample hydrogen yields into hydrogen areal densities. After subtraction of the substrate contribution to the hydrogen yield, organic mass surrogates were obtained from the aerosol hydrogen areal densities using the same protocols employed by Malm et al. (1994).

S-XRF Analysis of Samples

S-XRF of filters and impaction strips has been used for the past decade (Cahill et al. 1992; Reid et al. 1994) for high sensitivity elemental analysis of aerosol samples. S-XRF data were collected on Line 10.3.1 of the Advanced Light Source (ALS) at Lawrence Berkeley National Laboratory using a white beam of energy 4–18 keV. S-XRF was utilized because of its time efficiency in generating elemental profiles across the extended impactor strip samples and because the incident x-ray flux causes minimal sample alteration (Reid et al. 1994). S-XRF analysis of strip samples has been described elsewhere (Reid et al. 1994) and is summarized here. Briefly, strip samples were scanned with a beam spot size of 1×1 mm^2 and x-rays were detected with an energy dispersive Si(Li) x-ray detector located 5 cm from the sample. The beam dwelt at each point on a sample for 30 s before the sample was moved to the next location. With these parameters, a sensitivity of ~0.1 ng/m^3 for transition metals is achieved for the rotating drum sampler strips. Data reduction was performed offline using the well-accepted international XRF code AXIL, and profiles of elements with atomic number >10 were generated. The 1×1 mm^2 beam spot used to generate the S-XRF elemental profiles corresponds to an impactor drum collection time period of 6 h. Mass surrogates from the S-XRF element signatures were obtained using the same protocols employed by Malm et al. (1994).

Conversion from Areal Densities (μg/m^2) to Aerosol Concentration (μg/m^3)

To convert from areal density in μg/m^2 to aerosol concentration in μg/m^3, one has to multiply the areal density by a conversion constant in cm^2/m^3, the area of the surface impacted by the volume of air. In a filter, it is just the area of the filter divided by the volume of air samples. In a rotating drum impactor, the area is set by the rotation rate times the slit length. In this paper aerosol concentrations were calculated for a collection time period of 6 h, corresponding to a 1×6 mm area on a strip. Six hours of sampling at a flow of 10 L/min gives a volume of 3.6 m^3 (Cahill 1978). The resulting conversion constant is 0.0167 cm^2/m^3, about 4 times smaller than Interagency Monitoring of Protected Visual Environments Program (IMPROVE) (Malm et al. 1994).

Statistical Analysis

Relevant data sets were compared using linear regression analysis with the statistics software package GBSTAT. A coefficient of correlation (R^2) > 0.7 was considered to show significant correlation between data sets.

RESULTS AND DISCUSSION

Accuracy and Sensitivity of STIM in Determining Profiles of Aerosol Mass

STIM measurements shown in Table 2 from the 4 blank Apiezon-L coated Mylar strips reveal that incident 3 MeV protons lose ~50 keV in traversing the 480 μg/cm^2 films and that the energy loss over each of the 4 films is uniform to within 4 keV. Furthermore, during STIM and PESA analysis, the incident beam passes through the substrate before the deposited

Table 2
Average (mean ± standard deviation), minimum, and maximum STIM energy losses from each of 4 blank Apiezon-L coated Mylar films; data obtained from analysis of 90 contiguous 1 mm × 0.125 μm areas in a vertical linescan across each film

Film	Average energy loss (keV)	Minimum energy loss (keV)	Maximum energy loss (keV)
1	49.7 ± 0.5	48.4	51.7
2	49.4 ± 0.6	48.1	51.2
3	50.3 ± 0.5	48.8	51.5
4	50.7 ± 0.6	48.7	51.7

aerosol. This orientation ensures that the beam always loses the same amount of energy in passing through a uniform substrate independent of variations in the amount of aerosol on the sample. Consequently, the relative uniformity in energy thickness of the substrate enables the 50 keV energy loss arising from the substrate to be reliably subtracted from the energy losses arising from aerosol laden samples to produce profiles of energy loss solely arising from the deposited aerosols. The data in Table 2 suggest that the resulting energy loss arising solely from the aerosol should be accurate to within ±2 keV for each point in a profile. Confirmation of this inference was provided by looking at blank regions of each FACES sample. After applying the substrate energy loss correction of 50 keV, blank regions on each FACES sample had energy losses between −2 and 2 keV.

Figure 1 shows curves of areal density versus calculated proton energy loss for a 2.95 MeV proton beam passing through the aerosol composition shown in Table 1 and a $C_5H_9O_2N$ matrix (2.95 MeV corresponds to the proton beam energy after traversing the Apiezon-L coated Mylar film). The $C_5H_9O_2N$ matrix has been previously determined to be an accurate model (Lefevre et al. 1987, 1991; Bench et al. 1993) for proton energy losses in organic material, and changes of ±1 atom in C, H, N, and O content typically produce changes in areal density of <3% (Lefevre et al. 1987). The two curves in Figure 1 differ by <15%, illustrating the relative insensitivity of the stopping power curves to chemical composition. Consequently, in most instances the aerosol composition shown in Table 1 should yield an accuracy of better than 90% when used to convert energy losses to projected densities.

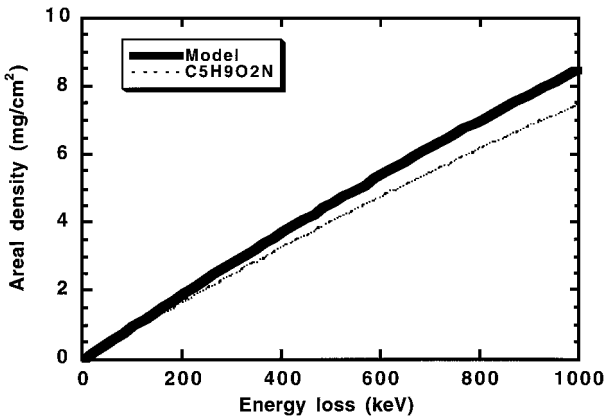

Figure 1. Curves of areal density versus proton energy loss for a 2.95 MeV proton beam passing through the aerosol composition shown in Table 1 and a $C_5H_9O_2N$ matrix.

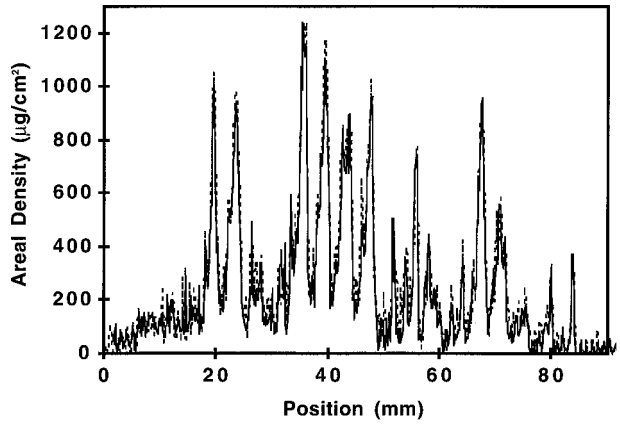

Figure 2. Two separate linescans (solid line and dashed line) of areal density versus position across the FACES rotating drum impactor stage 8 sample. The 2 linescans were separated by a horizontal distance of 2 mm.

Figure 2 shows the 2 separate STIM linescans of aerosol mass along the FACES stage 8 sample. Linear regression of the 2 data sets yields an $R^2 = 0.94$ and only minor differences in areal density for a given position are observed. The reproducibility in the data determined visually/graphically, together with signal to noise values in the 2 linescans, indicate an aerosol mass sensitivity approaching 10 μg/cm^2. Such a sensitivity compares favorably with theoretical calculations of areal density sensitivity of 10–30 μg/cm^2 for 3 MeV protons in low atomic number dominated matrices (Bench 1991). The mass sensitivity obtained with STIM could be improved by utilizing heavier ions or a lower proton beam energy (Bench et al. 1993). For example, use of a 2 MeV alpha particle beam could improve areal density sensitivity and resolution by an order of magnitude compared to 3 MeV protons (Bench et al. 1993). In principle, STIM would also lend itself well to making measurements of aerosol mass on Teflon or other thin films, providing the films have good areal density uniformity. However, in preliminary STIM scans of Teflon strips we have found that the areal density typically varies by 40% over the strip length. Such variation would presently preclude an accurate aerosol mass analysis by STIM.

Accuracy and Sensitivity of PESA in Determining Aerosol Hydrogen Profiles

The nominal hydrogen content in the Apiezon-L coated Mylar film determined from its thickness and composition is 20 μg/cm^2. PESA measurements of the blank Apiezon-L coated

Table 3
Average (mean ± standard deviation), minimum, and maximum PESA hydrogen masses from each of 4 blank Apiezon-L coated Mylar films; data obtained from analysis of 90 contiguous 1 mm × 0.125 μm areas in a vertical linescan across each film

Film	Average hydrogen content (μg/cm^2)	Minimum hydrogen content (μg/cm^2)	Maximum hydrogen content (μg/cm^2)
1	20.0 ± 0.2	19.4 ± 0.5	20.7 ± 0.5
2	20.2 ± 0.3	19.5 ± 0.5	20.8 ± 0.5
3	20.1 ± 0.2	19.1 ± 0.5	20.9 ± 0.5
4	19.8 ± 0.2	19.3 ± 0.5	20.5 ± 0.5

Mylar strips (Table 3) revealed the maximum variation in the hydrogen content across the analyzed region of each sample to be <10% of the average sample hydrogen content of ~20 mg/cm^2. This relative uniformity in hydrogen content of the film enables the hydrogen yields arising from the film to be reliably subtracted from the hydrogen yields arising from aerosol-laden samples to produce profiles of hydrogen yield solely arising from the deposited aerosols. The data in Table 3 further suggest that the resulting hydrogen yields arising solely from the aerosol should be accurate to within ±1 μg/cm^2 for each point in the profile. Confirmation of this inference was provided by looking at blank regions of each FACES sample. After subtracting the substrate contribution to the hydrogen yield blank regions on each FACES sample had hydrogen contents between −1 and 1 μg/cm^2. Consequently, the remaining data derived from PESA in this paper have been corrected for the substrate hydrogen contribution of 20 μg/cm^2.

Figure 3 shows the 2 separate PESA linescans of aerosol hydrogen mass along the FACES stage 8 rotating drum impactor sample. Linear regression of the 2 data sets yields an $R^2 = 0.92$, and only minor differences in hydrogen mass for a given position are observed. The reproducibility in the data determined visually/graphically, together with signal to noise values in the 2 linescans, indicates an aerosol hydrogen mass sensitivity of ~1 μg/cm^2. Such a sensitivity compares favorably with the sensitivity that can be calculated using the hydrogen yield data from the 4 blank Apiezon-L coated nylon strips. The hydrogen yield at each position ordinate in the resulting PESA profiles of the substrates was ~2000 counts or 100 counts/(μg/cm^2). Using the formulation that the minimum detectable hydrogen signal from the aerosols that can be resolved over the background contribution arising from the substrate is 3.29 times the square root of the substrate contribution (Currie 1968) yields 150 counts or 1.5 μg/cm^2 as the minimum detectable limit.

One other point worth noting is that since the hydrogen content within the Mylar substrate is 20 μg/cm^2, regions on the film that have not been exposed to aerosols could serve as an integral standard to convert aerosol hydrogen yields to hydrogen masses.

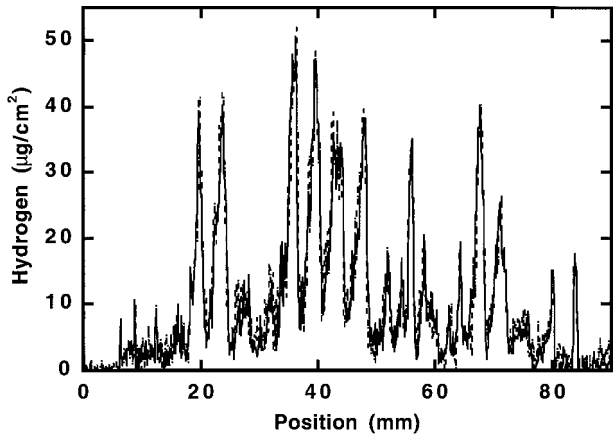

Figure 3. Two separate linescans (solid line and dashed line) of hydrogen mass versus position across the FACES rotating drum impactor stage 8 sample. The 2 linescans were separated by a horizontal distance of 2 mm.

STIM and PESA Profiles from the 6 FACES Sub $PM_{2.5}$ Mode Stages

Figure 4 shows STIM derived linescans of aerosol mass along the 6 FACES sub $PM_{2.5}$ mode stages. Similarly, Figure 5 shows PESA derived linescans of aerosol hydrogen mass along the same 6 FACES stages. It is not the purpose of this paper to present a detailed analysis of the aerosol science in these profiles, however, the STIM and PESA data from the 6 sub $PM_{2.5}$ modes show that dramatic changes in both total and hydrogen mass occur as a function of size and time in the various size fractions. The data also indicate that a surprisingly high fraction of the local $PM_{2.5}$ mass and organic matter is in very fine (stages 5 and 6) to ultra-fine (stages 7 and 8) modes with the ultra-fines representing a large fraction of the total fine mass (EPA 1995).

Integration of STIM and PESA with S-XRF Data

Again, it is not the purpose of this paper to present a detailed analysis of ambient aerosols of Fresno, but for completeness Figure 6 shows a comparison of some of the S-XRF data from the FACES stage 8 sample with the corresponding STIM and PESA data. The horizontal axis has been recalibrated so that it represents time and day of collection over the time period November 8 to 27, 2000. In the top graph, the STIM and PESA results from Figures 2 and 3 have been rebinned (data averaged over every block of 8 pixels) to have the same temporal resolution of 6 h as the S-XRF data. In addition the STIM and PESA mass per unit area data have respectively been converted to total aerosol mass and surrogate organic aerosol mass per cubic meter of air sampled using the protocols used by Malm et al. (1994).

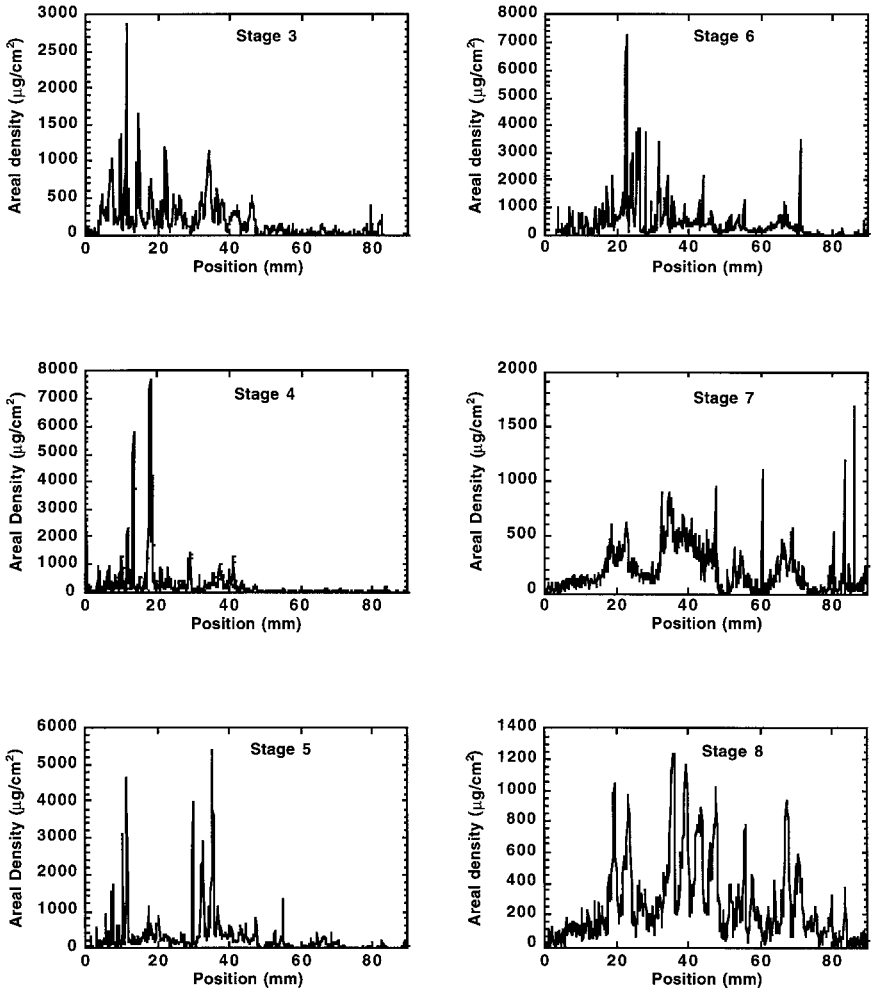

Figure 4. Linescans of aerosol mass versus position across the 6 FACES sub $PM_{2.5}$ mode rotating drum impactor stages (stages 3–8) analyzed by STIM. The average aerosol mass on each impactor stage was 190 μg/cm^2 for stage 3, 272 μg/cm^2 for stage 4, 277 μg/cm^2 for stage 5, 451 μg/cm^2 for stage 6, 193 μg/cm^2 for stage 7, and 262 μg/cm^2 for stage 8.

The middle graph displays S-XRF profiles of the trace elements copper, iron, and zinc, while the bottom graph presents S-XRF profiles of sulfur, chlorine, and potassism.

The top graph in Figure 6 indicates a high degree of correlation between the total aerosol mass and surrogate organic aerosol mass in the stage 8 sample. Figure 7 shows a graph of the regression of surrogate organic aerosol mass measured by PESA versus total aerosol mass measured by STIM. The coefficient of correlation between the mass measured by STIM and the organic matter measured by PESA is 0.81. Considering all the uncertainties in sampling and analysis and the dramatic changes in these parameters versus time, the agreement must be considered excellent. Integrating under the 2 curves in the top graph in Figure 6 indicates that ~45% of the total aerosol mass is comprised of organic matter. Closer inspection of the top graph in Figure 6 also suggests that the ratio of organic matter to total aerosol mass appears to be higher during the daytime than the nighttime. The fact that nonbiomass organic matter contributes a significant fraction to the ultra-fine particles in stage 8 in Fresno was previously unsuspected and raises important questions as to the nature of what low volatility organic species can survive Kelvin effect evaporation associated with such small diameter particles.

As with the STIM and PESA data, the elements with atomic number $\geq$11 in Figure 6 also change dramatically as a function of time. While iron is usually found in soils, the iron in this size mode has essentially no silicon (and little calcium) associated with it. This, plus its very fine size, indicates that it has an anthropogenic origin. Note the almost total lack of iron on the nights of November 22 and 23 when copper and zinc track the mass and organic species. Potassium can be associated with soil ($D_p > 1$ μm) and bio-mass smoke ($0.3 < D_p < 1$ μm). The potassium seen here is of neither source but is highly correlated with anthropogenic trace metals such as copper and zinc. The

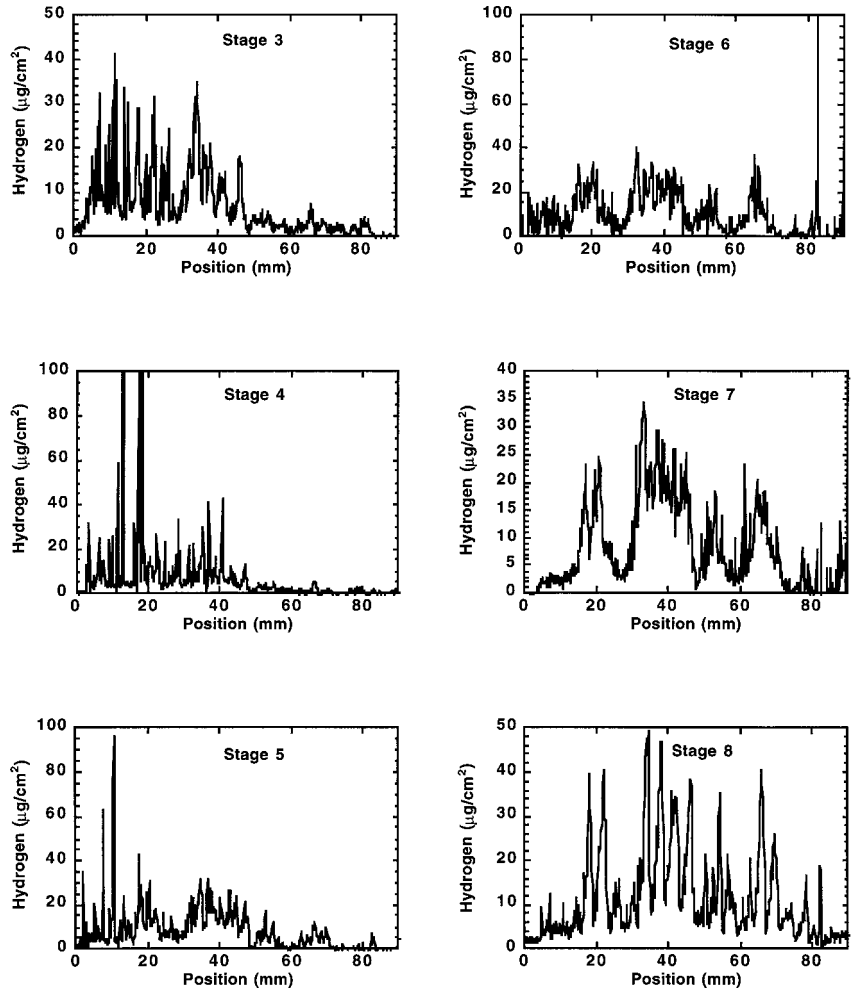

Figure 5. Linescans of aerosol hydrogen content versus position across the 6 FACES sub $PM_{2.5}$ mode rotating drum impactor stages (stages 3–8) analyzed by PESA. The average aerosol hydrogen mass on each stage was 6.8 $\mu g/cm^2$ for stage 3, 7.0 $\mu g/cm^2$ for stage 4, 7.7 $\mu g/cm^2$ for stage 5, 10.8 $\mu g/cm^2$ for stage 6, 8.3 $\mu g/cm^2$ for stage 7, and 11.6 $\mu g/cm^2$ for stage 8.

S-XRF data combined with the high correlation between the STIM and PESA results, and the fact that when converted into aerosol composition roughly 45% of the aerosol mass in the stage 8 FACES sample was organic, point to an unexpected ultra-fine organic aerosol in Fresno. These data, when combined with XRF data for trace elements, suggest a possible high temperature anthropogenic source such as diesel exhaust.

The data in Figures 4, 5, and 6 reveal a wealth of information unseen in analyses of $PM_{2.5}$ filters. Such data have the potential to be major assets in correlating aerosols and health impacts, visibility degradation, and the effects of aerosols on climate. Furthermore, owing to the dramatic changes in time for the elements sodium and heavier, the STIM mass and PESA organic surrogate mass provide crucial data in approaching mass closure. Reconstructed masses using the protocols of Malm et al. (1994) and the elemental signatures from the PESA and S-XRF analyses were compared to the total aerosol masses obtained by STIM for each of the 6 FACES sub $PM_{2.5}$ mode stages. The comparison suggests that mass closure for the coarse stages (stages 3 and 4), dominated by soils, is typically around 80%, similar to that reported in dry, western sites by the Interagency Monitoring of Protected Visual Environments (IMPROVE) program (Malm et al. 1994). This supports the absolute accuracy of mass by STIM, since a mass closure of around 80% is the typical result IMPROVE obtains using gravimetric mass. Mass closure in the finer stages (stages 5–8) is not possible presently because of the lack of data on nitrates, a major component in atmospheric fine mass in the San Joaquin Valley of California. However, the nuclear microprobe facility at Lawrence Livermore National Laboratory (LLNL) can measure nitrogen content in thin films via Rutherford back-scattering analysis, and Mylar is nitrogen-free. This opens the possibility of greatly increasing the fraction of mass observed. Initial measurements at the LLNL facility suggest that nitrogen contents in aerosol masses up to 500 $\mu g/cm^2$ collected on Mylar strips can be accurately measured via Rutherford back-scattering analysis.

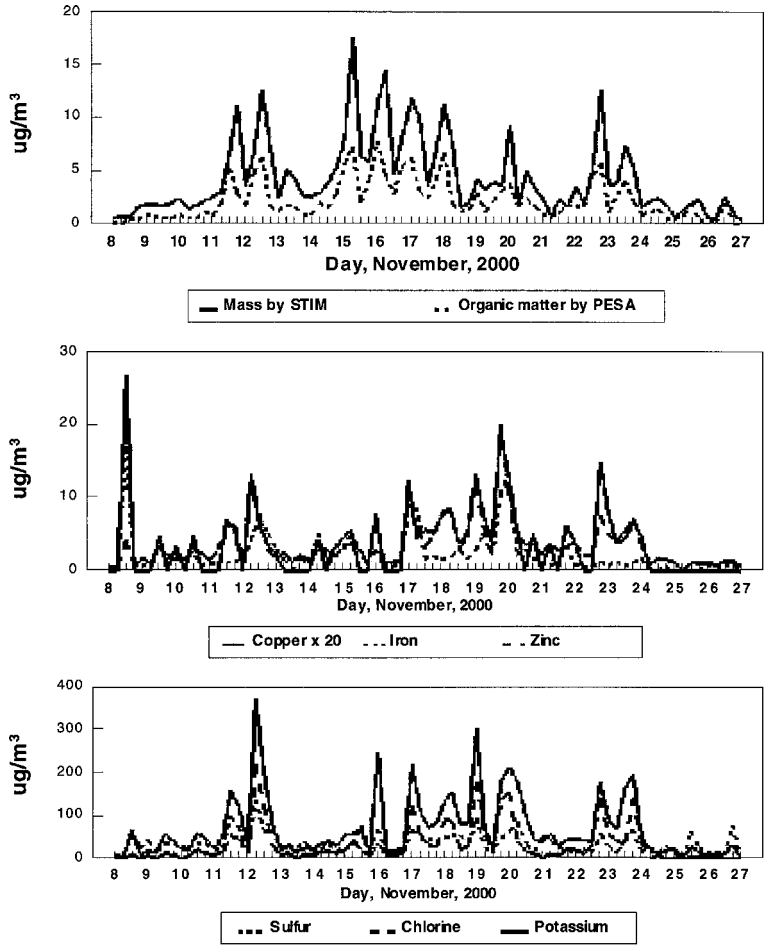

Figure 6. STIM, PESA, and S-XRF results from the FACES stage 8 rotating drum impactor sample. In the top graph, total aerosol mass (from STIM) and organic mass (from PESA) are presented. The middle graph presents 3 trace elements: copper, iron, and zinc. The bottom graph presents sulfur, chlorine, and potassium.

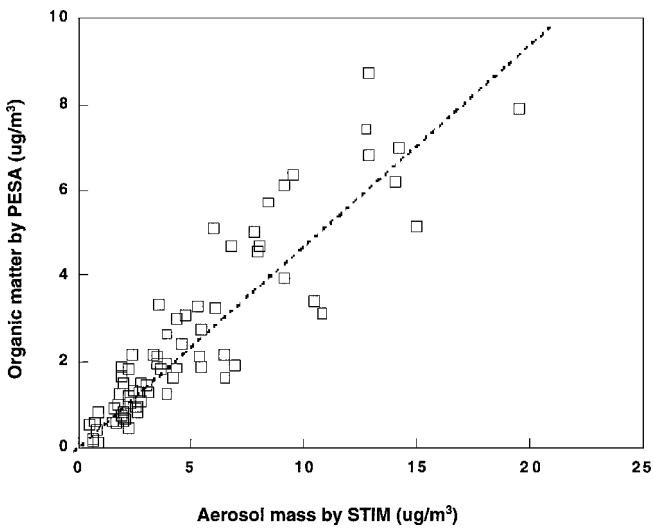

Figure 7. Graph of the regression of surrogate organic aerosol mass measured by PESA versus total aerosol mass measured by STIM from the FACES stage 8 rotating drum impactor sample.

CONCLUSIONS

In this study, we have established the ability of both STIM and PESA to provide hitherto unavailable information from the increasingly popular greased Mylar impaction stages. The STIM and PESA data from the Apiezon-L coated Mylar strips demonstrate that such samples possess excellent uniformity in thickness and hydrogen content, thus making them an ideal substrate for STIM analysis. The joining of such data with other techniques affords the ability to approach mass closure on size and time resolved aerosol samples.

REFERENCES

Barone, J. B., Cahill, T. A., Eldred, R. A., Flocchini, R. G., Shadoan, D. J., and Dietz, T. M. (1978). A Multivariate Statistical Analysis of Visibility Degradation at Four California Cities, *Atmos. Environ.* 12:2213–2221.

Bench, G. (1991). *Scanning Transmission Ion Microscopy*, Ph.D. thesis, University of Melbourne, Melbourne, Australia.

Bench, G. S., Saint, A., Legge, G. J. F., and Cholewa, M. (1993). Applications of Energy Loss Contrast STIM, *Nuclear Instruments and Methods in Physics Research B: Beam Interactions with Materials and Atoms* 77:175–183.

Cahill, T. A. (1978). Sensitivity, Quality Assurance, and Cost in Automated Analysis via Ion-Induced X-Rays, *Nuclear Instruments and Methods in Physics Research* 149:431–433.

Cahill, T. A. (1979). Comments on Surface Coatings for Lundgren-Type Impactors. In *Aerosol Measurement*, edited by D. A. Lundgren. University Presses of Florida, FL, pp. 131–134.

Cahill, T. A. (1996). Compositional Analysis of Atmospheric Aerosols. In *Particle-Induced X-Ray Emission Spectrometry*, edited by S. A. E. Johansson, J. L. Campbell, and K. G. Malmqvist. Chemical Analysis Series, John Wiley & Sons, Inc., New York, Vol. 133, 237–311.

Cahill, T. A., Eldred, R. A., Motallebi, N., and Malm, W. C. (1989). Indirect Measurement of Hydrocarbon Aerosols Across the United States by Non-sulfate Hydrogen-Remaining Gravimetric Mass Correlations, *Aerosol Sci. Technol*. 10:421–429.

Cahill, T. A., Eldred, R. A., Wallace, D., and Kusko, B. H. (1987). The Hydrogen-Sulfur Correlation, by PIXE Plus PESA, and Aerosol Source Identification, Fourth International PIXE Conference, Tallahassee, FL, June 9–13, 1986, *Nuclear Instruments and Methods in Physics Research B: Beam Interactions with Materials and Atoms* 22:296–300.

Cahill, T. A., and Wakabayashi, P. (1993). Compositional Analysis of Size-Segregated Aerosol Samples. In *Measurement Challenges in Atmospheric Chemistry*, edited by L. Newman. American Chemical Society, New York, Chapter 7, pp. 211–228.

Cahill, T. A., Wilkinson, K., and Schnell, R. (1992). Composition Analyses of Size-Resolved Aerosol Samples taken from Aircraft Downwind of Kuwait, Spring, 1991, *J. Geophys. Res.* 97(D13):145139–145150.

Cohen, D. D., Bailey, G. M., and Kondepudi, R. (1996). Elemental Analysis by PIXE and Other IBA Techniques and their Application to Source Fingerprinting of Fine Particle Pollution, *Nuclear Instruments and Methods in Physics Research B: Beam Interactions with Materials and Atoms* 109/110: 218–226.

Currie, L. A. (1968). Limits for Qualitative Detection and Quantitative Determination: Application to Radiochemistry, *Anal. Chem*. 40:586–593.

EPA (1995). *Criterion Document for Fine Particulate Matter*, EPA 600, Vol. 1, Section 6.

Flocchini, R. G., Cahill, T. A., Shadoan, D. J., Lange, S. J., Eldred, R. A., Feeney, P. J., Wolfe, G. W., Simmeroth, D. C., and Suder, J. K. (1976). Monitoring California's Aerosols by Size and Elemental Composition, *Environ. Sci. Technol.* 10:76–82.

Lefevre, H. W., Schofield, R. M. S., Bench, G., and Legge, G. J. F. (1991). STIM with Energy Loss Contrast: An Imaging Modality Unique to MeV Ions, *Nuclear Instruments and Methods in Physics Research B: Beam Interactions with Materials and Atoms* 54:363–370.

Lefevre, H. W., Schofield, R. M. S., Overley, J. C., and McDonald, J. C. (1987). Scanning Transmission Ion Microscopy as it Complements Particle Induced X-Ray Emission microscopy, *Scanning Microscopy* 1:879–889.

Malm, W. C., Sisler, J. F., Huffman, D., Eldred, R. A., and Cahill, T. A. (1994). Spatial and Seasonal Trends in Particle Concentration and Optical Extinction in the United States, *J. Geophys. Res.* 99(D1):1347–1370.

Raabe, O. (1997). *Personal communication*, Department for Health and the Environment, University of California, Davis.

Raabe, O. G., Braaten, D. A., Axelbaum, R. L., Teague, S. V., and Cahill, T. A. (1988). Calibration Studies of the DRUM Impactor, *J. Aerosol Sci.* 19(2):183–195.

Reid, J. S., Cahill, T. A., and Dunlap, M. R. (1994). Geometric/Aerodynamic Equivalent Diameter Ratios of Ash Aggregate Aerosols Collected in Burning Kuwaiti Well Fields, *Atmos. Environ*. 28(13):2227–2234.

Roberts, M. L., Grant, P. G., Bench, G. S., Brown, T. A., Frantz, B. R., Morse, D. H., and Antolak, A. J. (1999). The Stand-Alone Microprobe at Livermore, *Nuclear Instruments and Methods in Physics Research B: Beam Interactions with Materials and Atoms* 158:24–30.

Wesolowski, J. J., John, W., Devor, W., Cahill, T. A., Feeney, P. J., Wolfe, G., and Flocchini, R. (1978). Collection Surfaces of Cascade Impactors. In *X-Ray Fluorescence Analysis of Environmental Samples*, edited by T. Dzubay. Ann Arbor Science, Ann Arbor, MI, pp. 121–130.